Journal of Petroleum Science and Technology 11(2): 30, 2021 22-29
DOI:10.22078/jpst.2021.4626.1761

Journal of Petroleum Science and Technology

https://jpst.ripi.ir/

Geochemical Analysis of Shemshak Shale Formation in Gushfil Mine (Iran): Paleo-Depositional Environment and Organic Matter Thermal Maturity

Ziba Hosseini[1,2], Asadollah Mahboubi*[1], Reza Moussavi-Harami[1], Rudy Swennen[2], Mohamad Hosein Mahmudy-Gharaie[1] and Ahmad Khajehzadeh[3]

1. Department of Geology, Faculty of Science, Ferdowsi University of Mashhad, Mashhad, Iran

2. Department of Earth and Environmental Sciences, Faculty of Science, Katholieke Universiteit Leuven (KU Leuven), Leuven, Belgium

3. Research Institute of Petroleum Industry (RIPI), Tehran, Iran

Abstract

The present study investigated the geochemical characteristics of Shemshak shales as a probable oil source rock in the Gushfil mine located in the Sanandaj-Sirjan Zone (SSZ), Iran. Trace elements such as nickel, vanadium, chrome, molybdenum, and cobalt are used as paleoenvironmental indicators. Moreover, the ratio of these elements shows that oxic to disoxic conditions prevailed during the sedimentation period. The interrelation of these elements indicates that the upper part of Shemshak Formation of the Jurassic age was deposited in a terrestrial to the marine-terrestrial influenced environment. The solid bitumen reflectance (BR) documents that the black shales presently are overmature. Conjugation of BR and the insolubility of organic matter in carbon disulfide illustrates the presence of pyrobitumen and its subgroup epi- to meso-impsonite, which is also characterized by the absence of any fluorescence under ultraviolet light. The ratio of light to heavy hydrocarbons proves that the type of solid bitumen before pyro-bituminization has been a primary-oil solid bitumen, which could migrate through fractures and coarse pores. The primary-oil solid bitumen might be derived from Kerogen types II and III as documented by fibrous plant fragments, translucent phytoclasts and pollens. Presently, due to intense degradation, kerogen type IV dominates. The modeling confirms that a thermal degradation had probably occurred after the deposition of Lower Cretaceous carbonates when the shales were able to produce bitumen. Ultimately, intense hydrothermal degradation led the solid bitumen to evolve into pyrobitumen and caused the shales to evolve into a dry gas window.

Keywords: Shemshak Formation, Pyrobitumen, Trace Elements, Dry Gas, Thermal Modeling.

Introduction

The siliciclastic strata of the Shemshak Formation have outcrops in a wide range of Alborz, Central Iran and Sanandaj-Sirjan Zone (SSZ) [1]. It mainly consists of fine to coarse sandstones, siltstones, and shales with a high amount of carbonaceous shales and coal seams with a high potential for hydrocarbon generation [2-4]. This formation is deposited in a back-arc extensional tectonic regime, and it includes marine to terrestrial facies from Late Triassic to Middle Jurassic [3]. Shemshak strata attain an enormous thickness of up to 4000 m in Alborz, while it decreases toward SSZ [1,3]. The Shemshak Formation is considered the source rock for the Khangiran gas field in eastern Iran (Koppeh-dagh Zone). The oil and gas seepages in the Mazandaran area are also attributed to the organic-rich sediments of the Shemshak Formation, which are the main source rocks of hydrocarbon in the Alborz zone [5]. Despite the importance of this formation, only a few studies addressed the organic geochemistry and petrography of the Shemshak Formation in Alborz and Central Iran [2,4-6]. So far, no one has studied the black shales in the Sanandaj-Sirjan Zone (SSZ). Also, SSZ has numerous Zn-Pb deposits located in the Malayer-Esfahan Metallogenic Belt (MEMB). Some researchers argue that most of these ore deposits have been formed under the hydrocarbon effect, probably derived from the Shemshak black shales [7,8]. It means that hydrocarbon resources are important and play a fundamental role in metal accumulation. Hydrocarbons might act as transfer agent to carry metals (especially zinc) or the thermal maturity of the hydrocarbons can induce thermal sulfate reduction, which produces H_2S inducing ore formation [9,10]. However, the role of hydrocarbons in metal deposition cannot be constrained as long as the hydrocarbon source rock is not clearly defined in MEMB.

*Corresponding author: Asadollah Mahboubi, Department of Geology, Faculty of Science, Ferdowsi University of Mashhad, Mashhad, Iran
E-mail addresses: mahboubi@um.ac.ir
Received 2021-10-25, Received in revised form 2021-11-10, Accepted 2021-11-10, Available online 2021-12-08

The present study is carried out on black shales of the Gushfil mine located in the north flank of the Irankuh mine district (Figure 1). Irankuh is the biggest Zn-Pb deposit located 20 km southwest of Isfahan in MEMB which is situated within the SSZ structural plate. In the Gushfil area, black shales of the Shemshak Formation can be studied in outcrops, and they are present opposite to the dolostone host rocks along the Gushfil reverse fault. Our research investigated organic-rich shales as potential source rocks for hydrocarbons that occur in the Gushfil mine. The paleo-depositional environment of Jurassic black shales is constrained based on the use of trace elements. Furthermore, organic geochemistry is addressed, and the palynology of the shales is discussed. Our research investigates the geochemical properties (elemental and organic) of black shales and constructs a one-dimensional model of the burial history. Based on the latter, the maturation history and hydrocarbon production are addressed, contributing to a better understanding of these oil and gas source rocks.

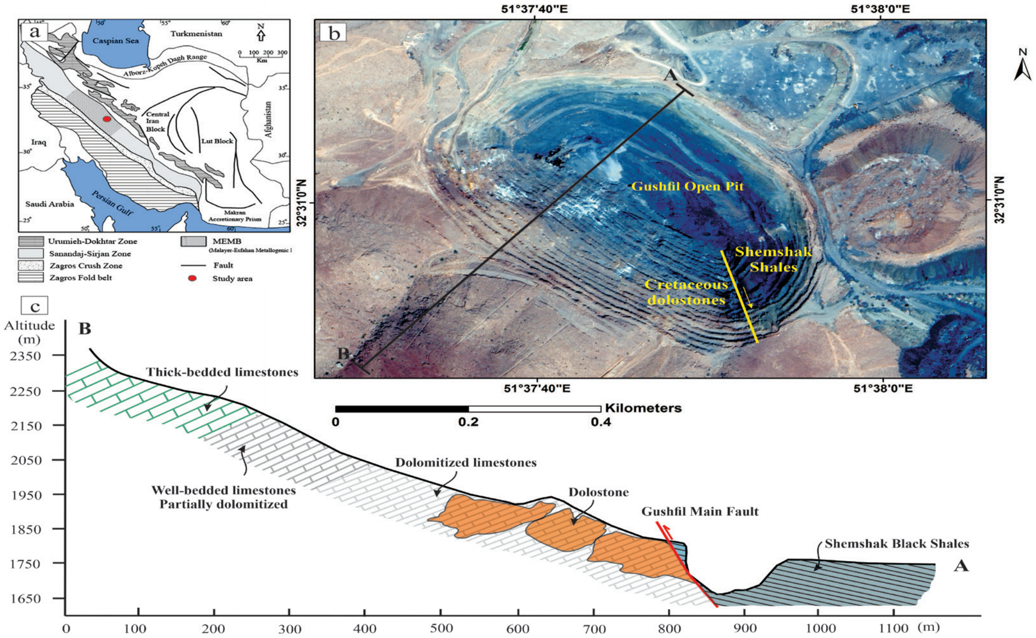

Fig. 1 Geological setting of our study area. a) Location of the Malyer-Isfahan Metallogenic-Belt (MEMB), Sanandaj-Sirjan Zone and Gushfil mine. b) Satellite map of the Gushfil mine, and c) Cross-section of the Gushfil ore hosting rocks modified after [11]. Position of cross-section is shown in b).

Geological Setting

The oldest rocks exposed in the Gushfil mine are siltstone and black shales with sandstone and calcareous interlayers belonging to Jurassic Shemshak Formation. This study deals with the shaly part of the Shemshak Formation, which displays an angular unconformity with Cretaceous carbonates of the Barremian-Aptian age. The thickness of the Shemshak Formation in this area is estimated as a maximum of 1500 meters thick [12], whereby more than half of it is composed of shales. This formation is deposited in a back-arc basin of the volcanic arc with a high geothermal gradient [1,13]. The Shemshak Formation also contains Triassic rocks, which were not considered in this study. The latter are exposed in the west of Isfahan (Tiran and Najaf-Abad regions); however, they were not drilled in Irankuh (south of Isfahan). Based on the observations of the present study, the accumulation of organic matter and coals in the drilling cores belonged to the boreholes drilled from inside the Gushfil pit. The deposited sediments after Shemshak Formation have a thickness of approximately 850 m, and they mainly consist of carbonates containing orbitolina, miliolida and rudist fossils. Most of these Cretaceous rocks were deposited in a shallow marine environment. After the Cretaceous, there is a gap in sedimentation and Irankuh was located in front of a volcanic arc due to the shift of the magmatic arc towards the Urmia-Dokhtar zone, which resulted in a lowering in geothermal gradient. Based on Re-Os dating of pyrites, the hydrothermal event occurred some 66.5±1.6 Ma ago [11], which links to zinc-lead ore emplacement in the Gushfil mine.

Materials and Methods

Thirty samples belonging to Shemshak shale Formation were collected from the Gushfil mine located in the northern flank of Irankuh. The samples originate from 2 boreholes drilled inside the Gushfil open pit and from the main tunnel of the Gushfil mine. They all belong to the upper part of the Jurassic Shemshak Formation. Samples were randomly taken perpendicular to the bedding. Ten polished uncovered thin sections, fifty palynology slides, and nine vitrinite blocks were prepared for the organic petrographical study. Thin section samples have been studied using an Olympus BX51 fluorescence microscope. The palynology slides were made after using the HCl/HF digestion method [14] from 4 samples that weighed about 150 grams. The percentage of solid bitumen reflectance (%BR) was measured with a Leitz MPV– COMBI reflected microscope attached to a PC-controlled software (TIDAS PMT IV system). Three samples were also analyzed for considering the amount of SARA (Saturate, Aromatic, Resin, and Asphaltene), which it was performed according to the standard ASTM D2007-03 (2008) method [15]. The organic matter (OM) was extracted using a Soxhlet apparatus with chloroform as an organic solvent.

Ethanol, n-C_5, and n-C_6 were used as eluent solvents, and the measurement error was less than 2%. The solubility of organic matter into an organic solvent (CS_2) was also investigated in portions of 1 gr OM to 10 cm^3 CS_2 with an incubation time of 24 hours. These experiments were carried out at RIPI (Research Institute of Petroleum Industry) and the Ferdowsi University of Mashhad. Furthermore, trace elements have been analyzed by ICP-OES in nine samples at KU Leuven (Belgium). The samples from non-mineralized intervals are faraway from the ores to prevent any possible effects of hydrothermal overprinting. They were prepared according to the four-acid digestion method including 3 ml HNO_3 (65%) + 1 ml $HClO_4$ (70%) + 3 ml HF (48%) + 7ml HCl (37%). The amount of powder was 100 grams per sample which, after dissolution, it was diluted to 25 ml with Milli-Q water, after which trace elements were measured using a Varian 720-ES machine. The one-dimensional modeling of the thermal history was carried out using PetroMod software.

Results and Discussion

The average reflectance of solid bitumen ranges from 1.8 to 2.7 for black shales of Shemshak Formation. This points to a dry gas to overmatured OM, which does not reflect any fluorescence light (Table 1). Vitrinite was not observed in the petrographic study. Therefore, the diagram presented in reference [16] has been used to equate the results of the solid bitumen reflectance (BR) to vitrinite reflectance (VR) (Figure 2). This diagram shows the results of BR based on references [17-24]. The calculated VR maturity of the samples has been plotted in the range of dry gas generation. It is noteworthy that these values were used to calibrate the thermal history model and the related interpretations. Due to the similarity of the reflection ranges of solid bitumen in the reference [23] with the present study, the exact values considered in the modeling are obtained from the equation (i.e. Equation 1) linking vitrinite reflectance to solid bitumen reflectance.

$$VR = (BR + 0.2443)/1.0495 \quad (1)$$

Table 1 Results of solid bitumen reflectance and calculated vitrinite reflectance.

Sample No.	Solid bitumen reflectance (BR%)			Equivalence of vitrinite reflectance (VR%)	Generation stage	Number of measurements	Standard deviation
	Min	Max	Mean				
1	2.02	2.74	2.32	2.44	Dry gas	19	0.26
2	2.15	2.51	2.33	2.45	Dry gas	12	0.14
3	2.03	2.75	2.36	2.48	Dry gas	10	0.24
4	1.92	2.62	2.22	2.35	Dry gas	14	0.23
5	2.04	2.90	2.47	2.58	Dry gas	15	0.29
6	2.10	2.60	2.35	2.47	Dry gas	9	0.18
7	1.63	2.10	1.84	1.98	Dry gas	14	0.12
8	2.12	2.94	2.68	2.90	Dry gas	8	0.28
9	2.31	3.19	2.66	2.81	Dry gas	16	0.25

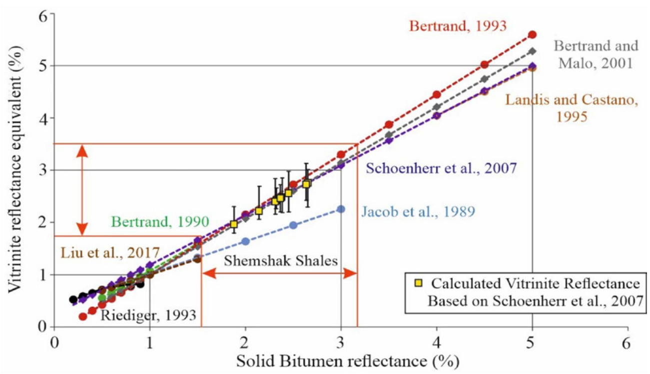

Fig. 2 Equivalence values of vitrinite reflectance calculated from the solid bitumen reflectance using the equation in reference [23].

The results of the SARA analysis are given in Table 2. The average percentage of asphaltene in the samples is approximately 35%. The total percentage of NSO components (Asphaltene + Resin) is more than 65%. The shale samples are in the naphthenic domain according to the reference classification [25].

The concentrations of nickel (Ni), vanadium (V), chromium (Cr), cobalt (Co), and molybdenum (Mo) from Shemshak shales are presented in Table 3. Vanadium has the highest concentration in six samples with an average of 76 ppm, whereas nickel shows a mean value of 62 ppm. Chromium and cobalt concentrations have mean values of 38, and 32 ppm, respectively and molybdenum has been detected in concentrations below 10 ppm (Table 3).

Table 2 Results of SARA (Saturate, Aromatic, Resin and Asphaltene) analysis from Shemshak shales in Gushfil mine.

Sample No.	Hydrocarbon structures				Asphaltene + Resin(%NSO)
	Saturate%	Aromatic%	Resin%	Asphaltene%	
1	15.2	14.9	35.7	34.2	69.7
2	15.8	16.6	31.5	36.1	67.6
3*	66.4			33.6	-

Table 3 Trace elements distribution from bulk shale samples in Gushfil mine.

Sample No.		1	2	3	4	5	6	7	8	9
Concentrations of trace elements	Ni	37	79	57	62	73	69	66	61	53
	V	84	125	24	20	13	127	103	101	89
	Cr	44	54	13	11	10	63	51	47	45
	Co	31	27	28	48	56	24	30	22	25
	Mo	1	7	1	0.9	0.7	6	4	8	1

The average solubility of OM into CS_2 is 25% which points to the pyrobitumen range with the existence of the sub-types Epi- and Meso-impsonite (Figure 3). Our palynology studies indicate different types of organic matter, as presented in Figure 4. A significant part, approximately 80%, is amorphous OM displayed as cloudy particles with color ranging from brown or even dark grey to black. The plant fragments and palynomorph group can be classified into different types, including opaque and semi-opaque particles, fibrous woody debris, translucent phytoclasts and a few spore pollens.

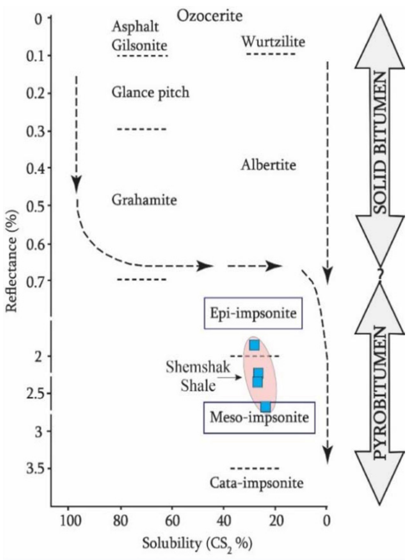

Fig. 3 Relationship between vitrinite reflectance and solubility in carbon disulphide (CS_2) modified after [17].

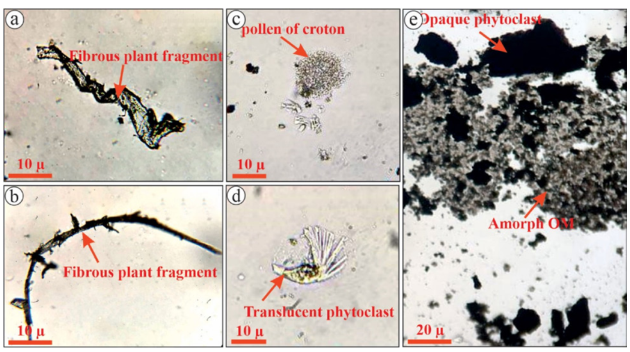

Fig. 4 Organic components in Shemshak shale Formation: a and b) Woody fragments with fibrous-looking; c and d) Internal fragments of terrestrial plant including a type of pollen and translucent phytoclasts; e) Amorphous OM with square and lath-shaped opaque particles derived from postdepositional alteration.

Geochemistry of Trace Elements

The trace elements, including V, Ni, Co, Cr, and Mo, can be used to reconstruct the paleo-environment [26,27]. Many studies have demonstrated that the ratios of V/Ni, Ni/Co and V/Cr are the important indicators to estimate paleo-redox conditions which are directly controlled by the depositional setting [28-29]. The V/Ni ratio increases in a reducing environment with values > 3, while ratios < 1.9 and between 1.9 to 3 represent oxic and sub-oxic environments, respectively [30]. For the upper Shemshak Formation, the V/Ni ranges between 0.2 and 2.3, which agrees with oxic to sub-oxic conditions. The concentrations of these two elements also reflect a terrestrial to the marine-terrestrial environment, as seen in Figure 5a. The concentration of cobalt in shales deposited under oxidizing conditions increases with the nickel concentration. In relatively oxidizing depositional conditions, the Ni/Co ratio will be less than 5 [31]. It means that Co is relatively enriched compared to Ni in oxic environments. The relationship between these two elements in the shaly samples of Shemshak shows that the amount of nickel is 3 times higher than that of cobalt, which is consistent with the results obtained from the V/Ni ratio. The Mo concentration increases under reducing conditions, and it is usually more than 5 ppm to about 40 ppm [32-36]. However, Mo in Shemshak shales is present in low amounts (Mo < 8 ppm), which also supports an oxic and sub-oxic setting. Chromium (Cr) is another important trace element to infer the paleo-depositional environment. If the V/Cr ratio is less than 2, it points towards oxic conditions at the time of sediment deposition [31]. This range was between 1.3 and 2.2 for Shemshak shales confirming oxic to sub-oxic conditions (Figure 5b). The results of our study are consistent with the geochemical results of Shemshak Formation in Dash-Aghol mine district [37]. According to the study from this deposit, Shemshak shales were deposited in an oxic environment, resulting from severe chemical weathering of the source material [37].

Organic Geochemistry

One of the most common methods to differentiate solid bitumen from pyrobitumen is the solubility of residual solid hydrocarbons (RSH) in carbon disulfide (CS_2). This method is known to determine solid bitumen and pyrobitumen sub-types when VR data are also available [17]. Accordingly, in Figure 3, it is shown that RSH from the Shemshak Formation is pyrobitumen, in the range of impsonite. The maturity of organic matter bears an inverse relationship with fluorescence [38]. The super-mature organic matter does not reflect ultraviolet light, which could justify why the shale samples are dark under fluorescence microscopy.

Pyrobitumen is a by-product of solid bitumen, which is produced due to intense thermal alterations. Solid bitumen trapped in the source rock by various heat sources (thermal gradient, magma infiltration or hydrothermal fluid infiltration) produces a secondary solid hydrocarbon type known as pyrobitumen [16,40].

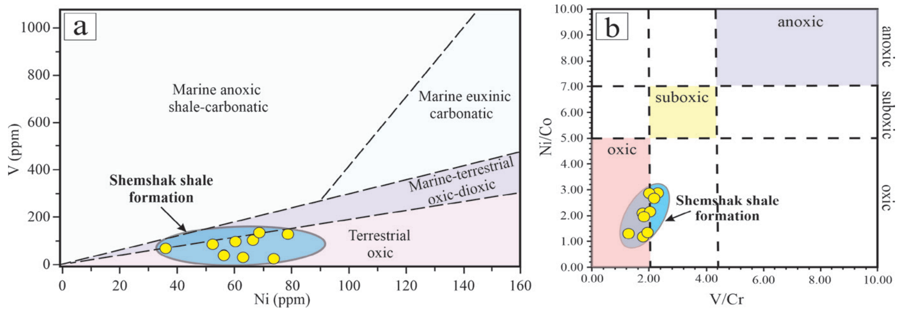

Fig. 5 Paleoenvironmental conditions are based on the concentration of trace elements. a) Cross-plot of V and Ni ratios displaying a terrestrial depositional environment for the Shemshak samples, b) Cross-plot of Ni/Co versus V/Cr indicating oxic to sub-oxic condition for the Shemshak samples.

In general, pyrobitumen shows a vitrinite reflection in the dry gas range, which it corresponds to the characteristics found in the Shemshak shale samples. This type of RSH can be seen in source or reservoir rocks. However, shale samples with a high level of asphaltene are more prone to generate pyrobitumen [39]. Porosity size in shales occurs mostly at nano- to micron scale. As a consequence, the high content of asphaltene can easily block the migration pathway for hydrocarbons.

In agreement with the latest classification [40], pyrobitumen can be produced as a by-product of three different types of solid bitumen placed in different thermal maturation stages, as seen in Figure 6. According to field studies and studies conducted in the Gushfil mine [8,41], migration of hydrocarbons to Lower Cretaceous dolostones has been observed in fractures and different types of secondary pores. Therefore, the origin of pyrobitumen in Shemshak Formation cannot be an initial-oil solid bitumen, which cannot migrate. SARA analysis shows that the average asphaltene content is 35%, and the approximate average of saturated hydrocarbons is 15%. These values indicate asphalts produced from a primary-oil solid bitumen [16,40]. The primary-oil solid bitumen has only the ability to migrate through large pores and fractures. Therefore, part of it remained in the organic-rich layers of Shemshak shale. The primary-oil solid bitumen, of which pyrobitumen is a by-product of its secondary thermal cracking in Gushfil, has originated from the solidification of hydrocarbons generated before reaching the oil window. The late-oil solid bitumen usually contains small amounts of asphaltene (less than 8%) [16,40], and it can migrate even through micro-pores. This type of solid bitumen does not correspond to the petrographic observations and the results of SARA analysis of our studied samples.

The results of palynology mostly show opaque phytoclasts and amorphous organic matters that demonstrate the presence of kerogen type IV. This result is in line with Rock-Eval results of Shemshak shales in the Gushfil mine [42]. Our palynology studies show the presence of fibrous plant fragments, translucent phytoclasts, and pollens which document that the primary source of kerogen type IV has been a mix of kerogen type II and III with a terrestrial to the marine-terrestrial source.

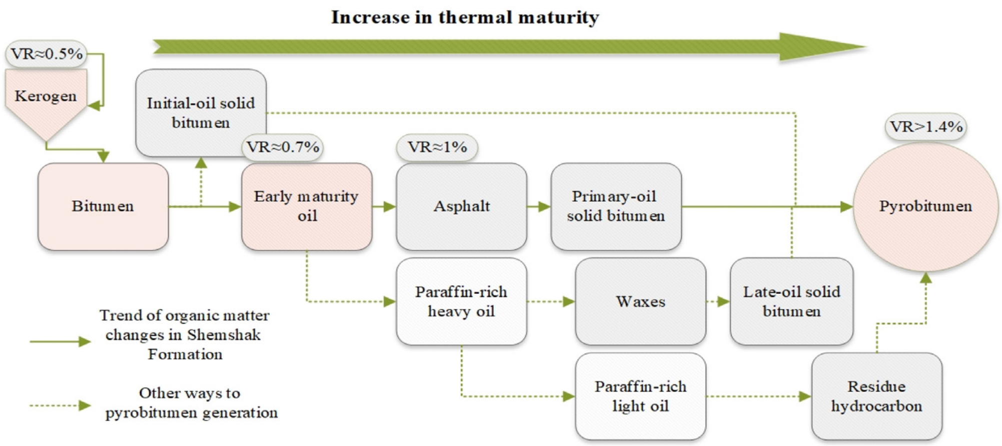

Fig. 6 Generation stages of pyrobitumen in Shemshak Formation based on the latest classification presented in reference [40].

Burial History Modeling

The source rock modeling aims to constrain better hydrocarbon generation, hydrocarbon maturity, and also petroleum migration. From the burial curves (Figure 7), it can be inferred that the maximum burial depth for Shemshak shales is less than 2500 meters. Using the available information on the thickness and depth of the layers, a hypothetical well is considered for modeling. The geothermal gradient, heat flow, age of formation and younger sub-formations, unconformities, and thickness of erosion were collected from previous studies [1,6,7,43]. Based on the tectonic setting, the heat flow is assumed to be 70-80 W/m^2 when Shemshak sediments are accumulated. Subsequently, it decreased to 40-35 W/m^2 in the Upper Cretaceous due to a change in the geodynamic setting of SSZ, which became placed in front of a volcanic arc (Fore-arc basin). The geothermal gradient is assumed to be 30 °C/km during the lower Jurassic, and it is considered to reach 18 °C/km in the Upper Cretaceous [8].

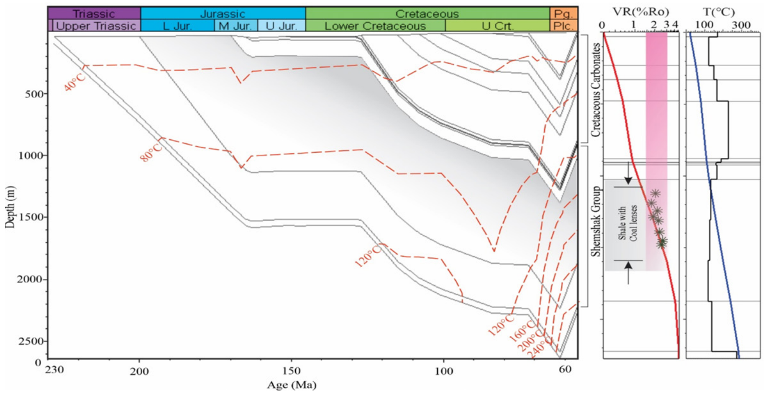

Fig. 7 One-dimensional modeling of Shemshak Formation located in Gushfil mine utilizing PetroMod software calibrated by vitrinite reflectance data (The black line in the temperature diagram indicates the heat transfer capability based on the rock type, and the blue line shows the average temperature of the sub-formations versus the depth. The increase in temperature in the Upper Cretaceous-Paleocene interval is related to the hydrothermal activity within the study area).

The software automatically adds the paleo-water depth and its temperature based on the age of formation and the latitude and longitude of the study area. The amount of erosion is calculated at about 350 meters based on younger sub-formations in the Irankuh anticline. After the Upper Cretaceous, no sediment was deposited, and so, this period is regarded as a gap in modelling. The development of the 1D burial history for the Gushfil mine indicates that the upper part of the Shemshak Formation has not been buried to depths greater than 2 Km (Figure 7). As can be observable, the Shemshak Formation could not generate hydrocarbons before sedimentation of Lower Cretaceous carbonates. Also, due to the petroleum migration of black shales to dolostone host rocks [6,8], the thermal source could not have happened in a syn-sedimentation setting with dolostones of the Barremian age. The high level of thermal maturity (VR ~2.5%) revealed that our samples were affected not only by the geothermal gradient, but also another thermal source that provided a secondary thermal cracking. The present study, which was conducted in a lead and zinc mine, suggests that the thermal maturation of organic matter is affected by the hydrothermal event in this area. As was mentioned above, the hydrothermal event happened near the Cretaceous-Tertiary (K-T) transition [11] based on the dating pyrites from the Irankuh main ore mineralization. Therefore, the model has been modified according to this time, and the temperature has been increased to maximum compliance with the vitrinite reflection data. The hydrothermal temperature is considered based on the reported temperatures of the fluid inclusions involved in reference [42], with a maximum of 240 °C and an average of 170 °C. During this period, Sanandaj-Sirjan was located in front of a volcanic arc, and it had a low geothermal gradient. However, the young oceanic crust could have played a significant role in fluid heating [8] and could have affected the thermal maturation of organic matter. Before thermal alteration, the upper part of Shemshak shales had reached a VR of 0.7%. This value is the minimum reflection in a primary-oil solid bitumen [40] which, based on our modeling, could only be provided after the deposition of the Upper Cretaceous successions. The age of the hydrothermal flux is consistent with the results presented in the section on organic geochemistry. The final burial history thus takes the hydrothermal flux into account, and it is well-matched with our vitrinite reflectance results.

Conclusions

This study provides inorganic and organic geochemical analyses to constrain the paleoenvironment setting and hydrocarbon potential of Shemshak Jurassic shales in the Gushfil mine located in southwest Esfahan (Iran). The concentration of trace elements such as vanadium (V), nickel (Ni), cobalt (Co), chromium (Cr), and molybdenum (Mo) has been investigated in non-mineralized rock intervals. The ratios of these elements demonstrate that the paleo-depositional environment of the Shemshak black shales has been a terrestrial to the marine-terrestrial environment. Black shales had been sedimented under oxic to sub-oxic conditions. Palynology analysis shows that shales could have generated kerogen type II and III. However, hydrothermal activity caused conversion to kerogen type IV. Shale samples containing pyrobitumen type Epi- to Meso-impsonite. The existing pyrobitumen was a secondary thermal by-product that resulted from the hydrothermal activity. This study indicates that the source of pyrobitumen is a primary-oil solid bitumen produced after deposition of Lower Cretaceous carbonates. The pyro-bituminization happened when Shemshak Formation had reached a vitrinite reflectance of 0.7%, equivalent to heavy oil production before the oil window. For further studies, organic geochemistry of Upper Triassic and Lower Cretaceous sub-formations is suggested.

Acknowledgment

This study was conducted as part of the Ph.D. thesis research of the first author at the Ferdowsi University of Mashhad (FUM)(#3/44367). We thank FUM for the support. The authors thank the Iran National Science Foundation for financial support of this research (Project No: 96013157). We wish to express our gratitude to the BAMA Company for providing the necessary facilities and to National Elites Foundation for allocating a laboratory grant. Also, we would like to express our great appreciation to Dr. Johan Fevery and his wife, Mrs. Maggy Rubens, for their help and valuable explanations and constructive suggestions during our study.

Nomenclatures

BR: Bitumen reflectance
OM: Organic matter
RSH: Residual solid hydrocarbons
SSZ: Sanandaj-Sirjan Zone
VR: Vitrinite reflectance

References

1. Hassanzadeh J, Wernicke BP (2016) The Neotethyan Sanandaj Sirjan zone of Iran as an archetype for passive margin arc transitions, Tectonics, 35, 3: 586-621.
2. Shekarifard A, Baudin F, Schnyder J, Seyed-Emami K (2009) Characterization of organic matter in the fine-grained siliciclastic sediments of the Shemshak Group (Upper Triassic–Middle Jurassic) in the Alborz Range, Northern Iran. In South Caspian to Central Iran Basins, , Geological Society, London, Special Publications, 312, 1: 161-174.
3. Fürsich F, Wilmsen M, Seyed-Emami K, Majidifard M (2006) The Upper Triassic-Middle Jurassic Shemshak Group of Iran: foreland basin or rift basin?, Volumina Jurassica, 4, 1: P. 41.
4. Shekarifard A, Baudin F, Seyed-Emami K, Schnyder J, Laggoun-Défarge F, Riboulleau A, Francoise Brunet M, Shahidi A (2012) Thermal maturity of the Upper Triassic–Middle Jurassic Shemshak Group (Alborz Range, Northern Iran) based on organic petrography, geochemistry and basin modelling: implications for source rock evaluation and petroleum exploration, Geological Magazine, 149, 1: 19-38.
5. Hamidi M, Fardoust F, Jafarzadeh M, Rabbani AR (2018) Organic geochemistry of the Upper Triassic–Middle Jurassic Shemshak Group (Alborz Mountains, NE Iran), Petroleum Science and Technology, 36, 21: 1764-1770.
6. Zamansani N, Rajabzadeh M A, Littke R, Zieger L, Baniasad A (2019) Organic petrology and geochemistry of Triassic and Jurassic coals of the Tabas Basin, Northeastern/Central Iran, International Journal of Coal Science and Technology, 6, 3: 354-371.
7. Ghazban F, McNutt R H, Schwarcz H P (1994) Genesis of sediment-hosted Zn-Pb-Ba deposits in the Irankuh district, Esfahan area, west-central Iran, Economic Geology, 89, 6: 1262-1278.
8. Karimpour M H, Sadeghi M (2018) Dehydration of hot oceanic slab at depth 30–50 km: KEY to formation of Irankuh-Emarat Pb Zn MVT belt, Central Iran, Journal of Geochemical Exploration, 194: 88-103.
9. Heydari E (1997) The role of burial diagenesis in hydrocarbon destruction and H2S accumulation, Upper Jurassic Smackover Formation, Black Creek Field, Mississippi, AAPG Bulletin, 81, 1: 26-45.
10. Sanz-Robinson J, Williams-Jones A E (2019) Zinc solubility, speciation and deposition: A role for liquid hydrocarbons as ore fluids for Mississippi Valley Type Zn-Pb deposits, Chemical Geology, 520: 60-68.
11. Liu Y, Song Y, Fard M, Zhou L, Hou Z, Kendrick M A (2019) Pyrite Re-Os age constraints on the Irankuh Zn-Pb deposit, Iran, and regional implications, Ore Geology Reviews, 104: 148-159.
12. Abdolahi M R, Jafarian M B, Goodarzi G, Pirhadi R, Partoazar H, Shahidi A, Navajari S (2013) 1:25000 geological map of south Esfahan, Geological Survey of Iran, Sheet No. 6355 III SE.
13. Mohajjel M, Fergusson C L)2014(Jurassic to Cenozoic tectonics of the Zagros Orogen in northwestern Iran, International Geology Review, 56, 3: 263-287.
14. Wood G D, Gabriel A M, Lawson J C (1996) Chapter 3. Palynological techniques -processing and microscopy. In: Jansonius J, McGregor D C (eds) Palynology: principles and applications. American Association of Stratigraphy Palynologists Foundation, Vol. 1. Publishers Press, Salt Lake City, Utah, USA, p. 29-50.
15. ASTM D2007 - 03, (2008) Standard Test Method for Characteristic Groups in Rubber Extender and Processing Oils and Other Petroleum-Derived Oils by the Clay-Gel Absorption Chromatographic Method, ASTM Committee on Standards, Philadelphia.
16. Mastalerz M, Drobniak A, Stankiewicz A B (2018) Origin, properties, and implications of solid bitumen in source-rock reservoirs: a review, International Journal of Coal Geology, 195: 14-36.
17. Jacob H (1989) Classification, structure, genesis and practical importance of natural solid oil bitumen (“migrabitumen”), International Journal of Coal Geology, 11, 1: 65-79.
18. Bertrand R (1990) Correlations among the reflectances of vitrinite, chitinozoans, graptolites and scolecodonts, Organic Geochemistry, 15, 6: 565-574.
19. Bertrand R (1993) Standardization of solid bitumen reflectance to vitrinite in some Paleozoic sequences of Canada, Energy Sources, 15, 2: 269-287.
20. Riediger C L (1993) Solid bitumen reflectance and Rock-Eval Tmax as maturation indices: an example from the “Nordegg Member”, Western Canada Sedimentary Basin, International Journal of Coal Geology, 22, 3-4: 295-315.
21. Landis C R , Castaño J R (1995) Maturation and bulk chemical properties of a suite of solid hydrocarbons, Organic Geochemistry, 22, 1: 137-149.
22. Bertrand R, Malo M (2001) Source rock analysis, thermal maturation and hydrocarbon generation in Siluro-Devonian rocks of the Gaspe Belt basin, Canada, Bulletin of Canadian Petroleum Geology, 49, 2: 238-261.
23. Schoenherr J, Littke R, Urai J L, Kukla P A, Rawahi Z (2007) Polyphase thermal evolution in the Infra-Cambrian Ara Group (South Oman Salt Basin) as deduced by maturity of solid reservoir bitumen, Organic Geochemistry, 38, 8: 1293-1318.
24. Liu B, Schieber J, Mastalerz M (2017) Combined SEM and reflected light petrography of organic matter in the New Albany Shale (Devonian-Mississippian) in the Illinois Basin: A perspective on organic pore development with thermal maturation, International Journal of Coal Geology, 184: 57-72.
25. Tissot B P, Welte D H)1984(Petroleum Formation and Occurrence. A New Approach to Oil and Gas Exploration, Springer-Verlag, Berlin, 538.
26. Adegoke A K, Abdullah W H, Hakimi M H, Yandoka B M S, Mustapha K A, Aturamu A O (2014) Trace elements geochemistry of kerogen in Upper Cretaceous

sediments, Chad (Bornu) Basin, northeastern Nigeria: Origin and paleo-redox conditions, Journal of African Earth Sciences, 100: 675-683.
27. Togunwa O S, Abdullah W H (2017) Geochemical characterization of Neogene sediments from onshore West Baram Delta Province, Sarawak: Paleoenvironment, source input and thermal maturity, Open Geosciences, 9, 1: 302-313.
28. Bechtel A, Gratzer R, Sachsenhofer R F (2001) Chemical characteristics of upper Cretaceous (Turonian) jet of the Gosau group of gams/hieflau (styria, Austria), International journal of coal geology, 46 1: 27-49.
29. Lewan M D (1984) Factors controlling the proportionality of vanadium to nickel in crude oils, Geochimica et Cosmochimica Acta, 48, 11: 2231-2238.
30. Galarraga F, Reategui K, Martïnez A, Martínez M, Llamas J.F., Márquez G. (2008) V/Ni ratio as a parameter in palaeoenvironmental characterisation of nonmature medium-crude oils from several Latin American basins, Journal of Petroleum Science and Engineering, 61, 1: 9-14.
31. Jones B, Manning D A (1994) Comparison of geochemical indices used for the interpretation of palaeoredox conditions in ancient mudstones, Chemical Geology, 111, 1-4: 111-129.
32. Piper D Z (1994) Seawater as the source of minor elements in black shales, phosphorites and other sedimentary rocks, Chemical Geology, 114, 1-2: 95-114.
33. Crusius J, Calvert S, Pedersen T, Sage D (1996) Rhenium and molybdenum enrichments in sediments as indicators of oxic, suboxic and sulfidic conditions of deposition, Earth and Planetary Science Letters, 145, 1-4: 65-78.
34. Alberdi-Genolet M, Tocco R (1999) Trace metals and organic geochemistry of the Machiques Member (Aptian–Albian) and La Luna Formation (Cenomanian–Campanian), Venezuela, Chemical Geology, 160, 1-2: 19-38.
35. Akinlua A, Adekola S A, Swakamisa O, Fadipe O A, Akinyemi S A (2010) Trace element characterisation of Cretaceous Orange Basin hydrocarbon source rocks, Applied Geochemistry, 25, 10: 1587-1595.
36. Piper D Z, Calvert S E (2009) A marine biogeochemical perspective on black shale deposition, Earth-Science Reviews, 95, 1-2: 63-96.
37. Abedini A (2016) Geochemistry of shales of the Shemshak Formation of the Dash-Aghel mining district, Bukan, NW Iran: Provenance, source weathering, paleo-oxidation conditions, and tectonic setting, Sedimentary facies, 9, 2: 55-74.
38. Engel M H, Macko S A (2013) Organic geochemistry: principles and applications (2th ed.), Springer Science and Business Media, 11: 1-861.
39. Misch D, Gross D, Hawranek G, Horsfield B, Klaver J, Mendez-Martin F, Urai J L, Vranjes-Wessely S, Sachsenhofer R F, Schmatz J, Li J, Zou C (2019) Solid bitumen in shales: Petrographic characteristics and implications for reservoir characterization, International Journal of Coal Geology, 205: 14-31.
40. Sanei H (2020) Genesis of solid bitumen, Scientific Reports, 10, 1: 1-10.
41. Esmaeili Sevieri A, Karimpour M H, Malekzadeh Shafaroudi A, Mahboubi A, Song Y (2019) Irankuh lead-zinc mining district, southern Isfahan, Iran: Evidences of geology, fluid inclusion and isotope geochemistry, Periodico di Mineralogia, 88: 277-296.
42. Hosseini Z (2021) Petrography and geochemistry study of Cretaceous limestone and dolomites as lead-zinc host rock in Irankuh mine (South Isfahan), Unpublished report for Iran National Science Foundation, 50.
43. Hosseini-Dinani H (2016) Investigation on the lithogeochemical haloes of major, minor and trace elements in the host rocks, ore body, gossan and soil at Irankuh Zn – Pb district, southwest of Isfahan, PhD dissertation, Shahid Bahonar University of Kerman, 1-292.